

Heavy Flavour Physics at HERA

Beate Naroska¹

*University of Hamburg
II. Institut für Experimentalphysik
Luruper Chaussee 149
D 22761 Hamburg
E-mail: naroska@mail.desy.de*

Abstract. New results with increased statistics are presented for heavy flavour production at $Q^2 \lesssim 150 \text{ GeV}^2$ and in the photoproduction limit $Q^2 \rightarrow 0$. Cross sections for D^* production, F_2^c , the gluon density in the proton, and inelastic J/ψ production are discussed and compared to theoretical calculations. A first measurement of the $b\bar{b}$ cross section is reported.

Introduction

At HERA positrons of 27.5 GeV collide with 820 GeV protons yielding a center of mass energy of 300 GeV. Heavy flavours are predominantly produced in pairs by photon gluon fusion. Charm quark production is expected to be a factor 200 more abundant than bottom quarks at this energy. Heavy flavour processes give new opportunities of studying perturbative QCD at center of mass energies roughly a factor 10 higher than in fixed target experiments.

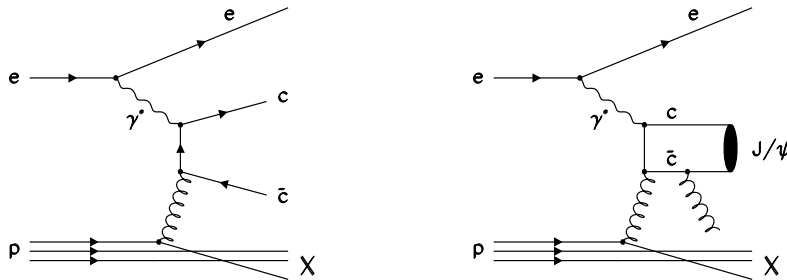


FIGURE 1. Charm production via photon gluon fusion (left) and J/ψ production in the color singlet model.

¹) Contribution to “Workshop on Heavy Quarks at Fixed Target”, Fermi National Accelerator Laboratory, Oct. 10, 1998

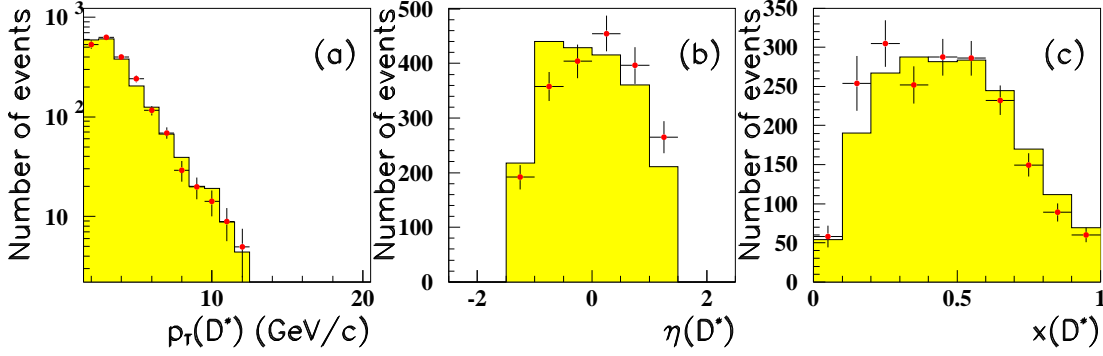


FIGURE 2. ZEUS: Reconstructed D^* related quantities compared to Monte Carlo simulation RAPGAP [2].

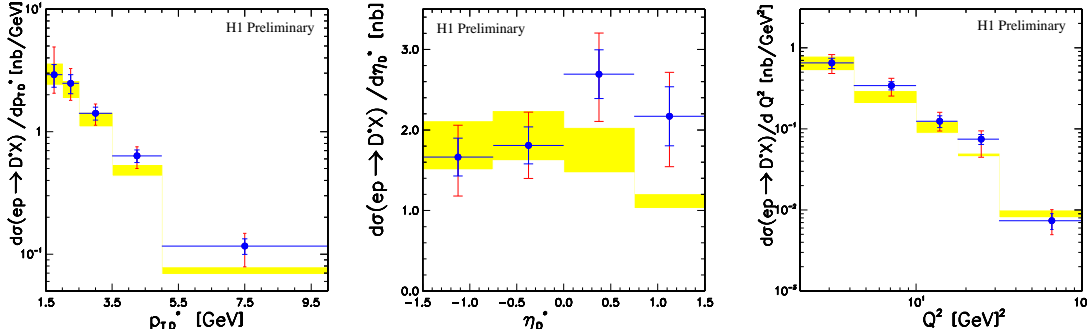


FIGURE 3. H1: Cross sections ($2 < Q^2 < 100 \text{ GeV}^2$, $0.05 < y < 0.7$, $p_T^{D^*} > 1.5 \text{ GeV}$, $|\eta^{D^*}| < 1.5$) compared to NLO calculations [3]. The shaded band represents the uncertainty in m_c .

There are several methods to tag heavy flavours: “Open” charm production is tagged via reconstruction of D^* (H1 and ZEUS) or via semi-leptonic decays to electrons (ZEUS). b quarks have been measured via semi-muonic decays by H1. Finally “hidden” charm is studied via reconstruction of J/ψ (see fig. 1). $\psi(2s)$ and Υ Mesons have as yet been reconstructed only in diffractive processes [1a] at HERA and will not be reported here.

The integrated luminosity delivered by HERA has steadily increased over the years. This review will cover data from 1995 ($\sim 6 \text{ pb}^{-1}$), 1996 ($\sim 10 \text{ pb}^{-1}$) and 1997 ($\sim 26 \text{ pb}^{-1}$). Most results are preliminary.

The usual kinematic variables for deep inelastic scattering are used:

$$s = (k + P)^2; Q^2 = -(k - k')^2; x = \frac{Q^2}{2P \cdot q}; y = \frac{q \cdot P}{k \cdot P}; W_{\gamma p}^2 = (q + P)^2 = sy - Q^2$$

where k and P are the four vectors of incoming electron and proton, and q of the exchanged photon.

Determination of F_2^c

The inclusive cross section for production of charm in deep inelastic scattering (DIS) can be written as

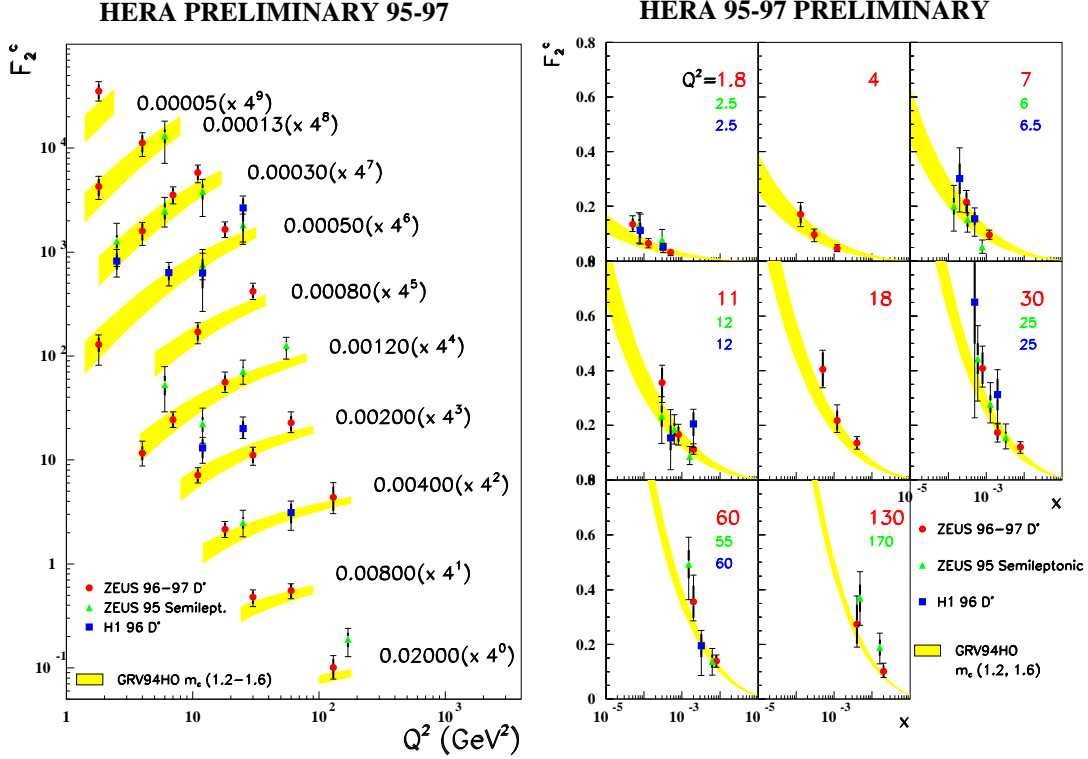


FIGURE 4. F_2^c as function of Q^2 at fixed x (scale factors applied for clarity); F_2^c as function of x in bins of Q^2 . For comparison a NLO prediction using the GRV94HO parton densities is shown with the uncertainty due to the charm mass.

$$\frac{d^2 \sigma^{ep \rightarrow e c \bar{c} X}}{dx dQ^2} = \frac{2\pi\alpha^2}{xQ^4} (1 + (1-y)^2) \cdot F_2^c(x, Q^2)$$

where the contribution due to F_L has been neglected since it is expected to be small.

Charm is tagged through reconstruction of $D^{*+} \rightarrow D^0 \pi^+$ with subsequent decay $D^0 \rightarrow K^- \pi^+$ and also the charge conjugate decay. ZEUS has presented a new analysis of semileptonic charm decays $c \rightarrow e^+ + X$. The electron was identified using the electromagnetic calorimeter and the specific energy loss dE/dx in the driftchamber. Details of the analysis from H1 and ZEUS can be found in [1b].

For D^* production a comparison to the RAPGAP Monte Carlo [2] simulation is shown in fig. 2. Reasonable agreement is found. After unfolding detector effects cross sections are obtained in a restricted kinematical region, examples from H1 data are shown in fig. 3. The data are compared to a NLO calculation by Harris and Smith [3] using the Peterson fragmentation function. The agreement is good and the extrapolation to the full kinematic region is done with this calculation.

The resulting Q^2 and x dependence of F_2^c is shown in fig. 4. The data span Q^2 values from 1.8 to 130 GeV^2 and $5 \cdot 10^{-5} \leq x \leq 0.02$. The agreement of the different

data sets is reasonable within errors. Also shown is the theoretical NLO calculation using the GRV94-HO parton density functions which reproduces the data well. A strong rise of F_2^c towards low x is observed at fixed Q^2 and in Q^2 strong scaling violations are seen at fixed x . F_2^c gives a contribution of between 10% (low Q^2) and 30% (high Q^2) to the inclusive F_2 at an $x \sim 5 \cdot 10^{-4}$.

Photoproduction of D^*

When the exchanged photon is almost real, contributions due to its hadronic nature have to be taken into account (“resolved” processes). In NLO QCD calculations an unambiguous separation of the direct process (fig. 5a) and resolved processes (b and c) is no longer possible, only the sum of the two is well defined. There are two approaches to calculate the photoproduction cross sections in next to leading order:

The “massive” approach [4] where only the light quarks u, d and s and gluons are active partons in the photon (and proton). Charm is only generated in the hard subprocess (see also fig. 5b). This approach is valid for $m_c \gg \Lambda_{QCD}$. The “massless” approach [5,6] where also charm is an active flavour. This approach is valid at $p_t \gg m_c$.

The high statistics data from ZEUS [7] are shown in fig. 6. They are found to be above the massive and massless calculations. The comparison of H1 data [1b] with massive calculations shown in fig. 7 is satisfactory.

ZEUS has presented an analysis of D^* events which contain two jets [7]. In these events the *observed* momentum fraction x_γ^{obs} can be calculated, which describes the fraction of the photon energy contributing to the production of the two jets. A significant tail at low x_γ^{obs} is found in the data. In the generator HERWIG this tail can be described by charm excitation in the photon, while considering only light flavours leads to discrepancies.

Gluon density from D^* events

H1 extracted the proton’s gluon density function in DIS ($2 < Q^2 < 100 \text{ GeV}^2$, $0.05 < y < 0.7$) and in photoproduction ($0.02 < y < 0.32$; $0.29 < y < 0.62$; $Q^2 \sim 0$) [1b].

The observed momentum fraction x_g^{obs} of the gluon is reconstructed from the kinematics of the final state and a differential cross section $d\sigma/dx_g^{obs}$ is determined, which for the DIS data is shown in fig. 8. The correlation of x_g^{obs} with the true x_g as given by the NLO QCD calculations [3] – also shown in fig. 8 – is used in an iterative unfolding procedure to obtain $d\sigma/dx_g$. The gluon density is then obtained by reweighting the calculation with the measured cross section. The result is shown in fig. 8 as a momentum distribution $x_g \cdot g(x_g)$. The range $10^{-3} < x_g < 0.02$ is covered. The data from photoproduction and DIS agree well within the large errors.

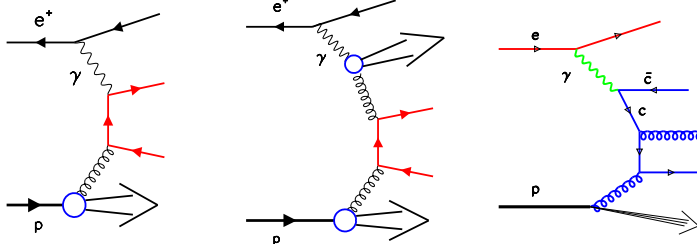


FIGURE 5. Generic diagrams for a) direct, b) resolved charm production. In c) a NLO diagram is shown (flavour excitation).

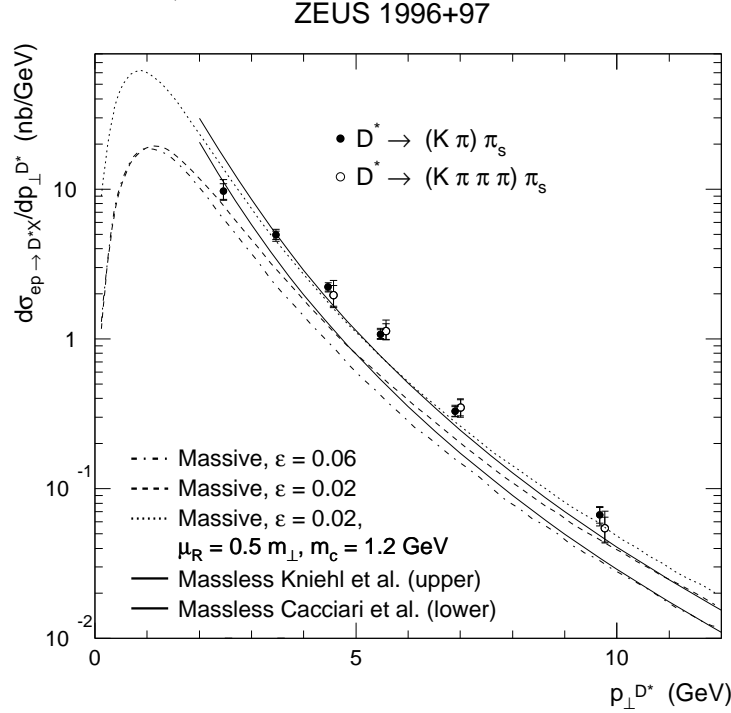


FIGURE 6. $d\sigma/dp_{\perp}$ for D^* photoproduction from ZEUS for $130 < W_{\gamma p} < 280$ GeV, $Q^2 < 1$ GeV² and $|\eta^{D^*}| < 1.5$ (η^{D^*} is the pseudorapidity of the D^*) for the $(K\pi)\pi$ and $(K\pi\pi\pi)\pi$ channels. The curves represent “massless” and “massive” calculations as indicated.

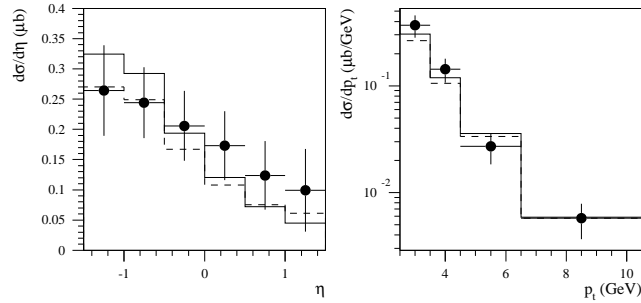


FIGURE 7. Photoproduction of D^* from H1: $d\sigma^{\gamma p}/d\eta$ for $p_{\perp} > 2.5$ GeV and $d\sigma^{\gamma p}/dp_{\perp}$ for $|y^{D^*}| < 1.5$, where y^{D^*} is the rapidity. The histograms show the NLO QCD predictions calculated according to [4] with the MRSG (solid) and MRSA' (dashed) proton parton density parametrizations.

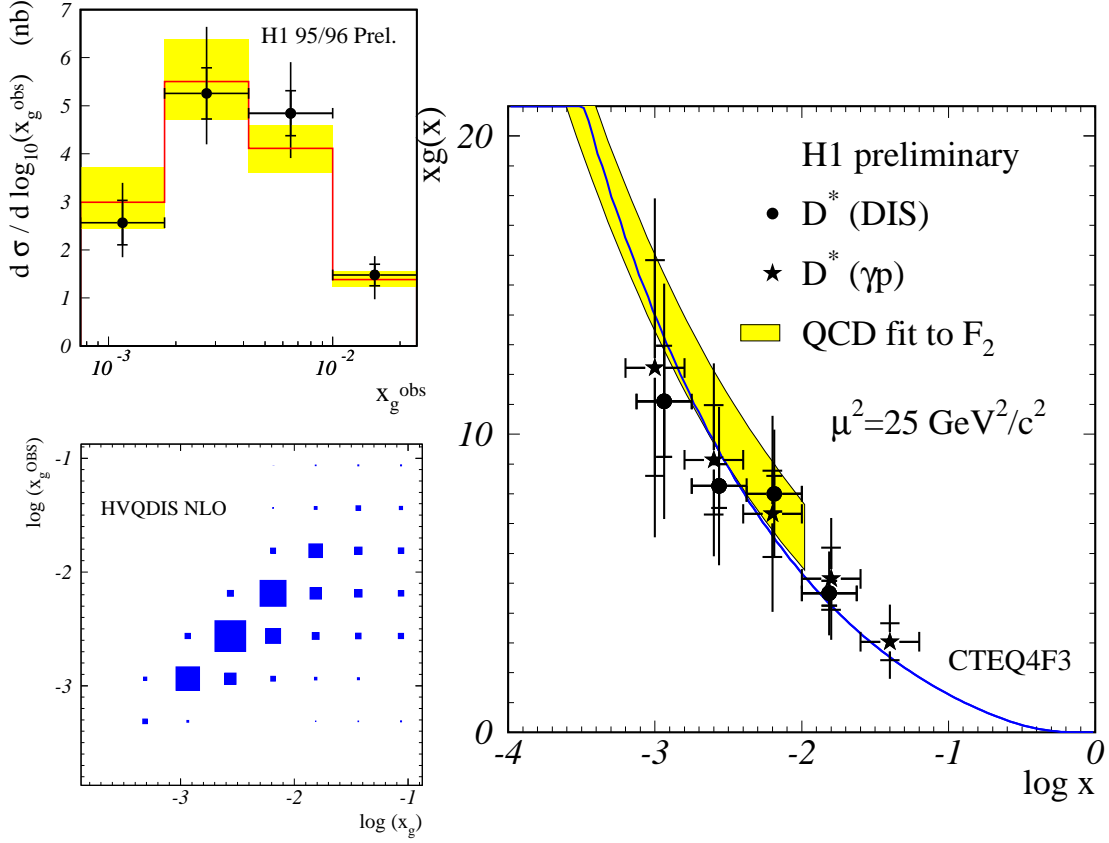


FIGURE 8. (a) Differential cross section for $ep \rightarrow eD^*X$ as function of x_g^{obs} in the visible range compared to the NLO QCD prediction using the CTEQ4F3 parton distribution. The shaded band reflects the uncertainty due to the charm mass $1.3 < m_c < 1.7 \text{ GeV}$. (b) Correlation between x_g^{obs} and true momentum fraction x_g . (c) Comparison of the gluon densities obtained from the two D^* analyses in DIS and photoproduction. The systematic error is dominated by the uncertainty of the charm quark mass and the fragmentation parameter. For comparison the H1 QCD analysis of the inclusive F_2 measurement (shaded band) and the CTEQ4F3 parametrization are shown.

They also agree with the result from an analysis of scaling violations in the inclusive measurement of F_2 [8].

$b\bar{b}$ Production

Due to the higher mass of the b quark the total cross section for $b\bar{b}$ production is expected to be 200 times smaller than that for $c\bar{c}$ production. The theoretical uncertainties in calculating the next to leading order predictions are, however, smaller [9]. H1 determined the cross section for the first time in the HERA energy range using semi-muonic b decays [1c].

A photoproduction event sample was selected containing two jets of transverse energy $E_T > 6 \text{ GeV}$ and a muon of transverse momentum (relative to the beam

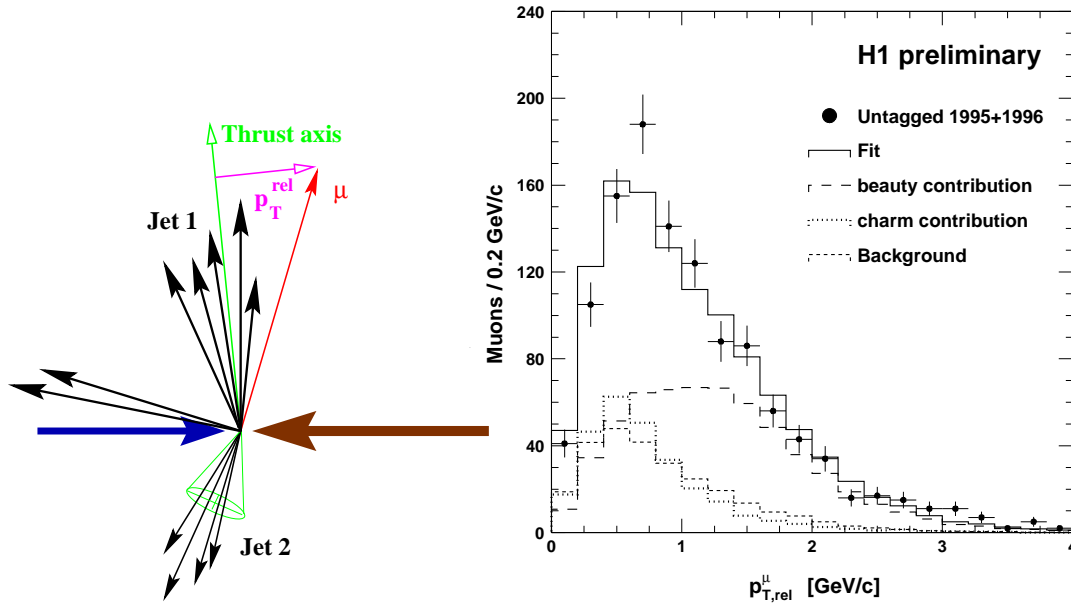


FIGURE 9. *Left:* Definition of $p_{T,rel}^\mu$. *Right:* The measured $p_{T,rel}^\mu$ distributions and the result of the fit (solid line); the contributions from beauty, charm and background are shown separately.

direction) $p_T^\mu > 2$ GeV in the central detector region $35^\circ < \theta^\mu < 130^\circ$.

The thrust axis² was determined for each jet in order to approximate the b flight direction. The transverse momentum of the muon $p_{t,rel}^\mu$ with respect to the jet is used as a discriminating variable: Muons from b decay show a $p_{t,rel}^\mu$ spectrum extending to higher values than c decays (see fig. 9 for an illustration of the method).

The background comes from the production of the light quarks u, d and s , which is roughly a factor 2000 larger than b production. Punch through and decay in flight lead to false muon signatures. The contribution is determined from data using an independent dataset and using the muon fake probability and the hadron composition from a well tuned and checked simulation program. The resulting $p_{t,rel}^\mu$ spectrum is shown in fig. 9 indicating the background contribution (23.5%), which is absolutely determined. The fractions of b and c quarks are obtained from a fit to the data distribution, yielding $(51.4 \pm 4.4)\%$ and $(23.5 \pm 4.3)\%$, respectively.

The cross section in the visible kinematic range of $Q^2 < 1$ GeV²; $p_T^\mu > 2$ GeV; $95 \leq W_{\gamma p} \leq 270$ GeV; $35^\circ < \theta^\mu < 130^\circ$ is determined as

$$\sigma(ep \rightarrow e b\bar{b} + X)^{vis} = 0.93 \pm 0.08_{-0.12}^{+0.21} \text{ nb},$$

where the first error is statistical and the second systematic. Contributions to the systematic errors are the branching ratio $b \rightarrow X\mu\nu$, the energy scale of calorimeters and detector efficiencies.

²⁾ The thrust axis is the axis which maximizes $T = \max(\frac{\sum p_i^L}{\sum |p_i|})$, where the sum runs over all particles belonging to the jet and p_i^L is the component of the particle momentum parallel to the thrust axis.

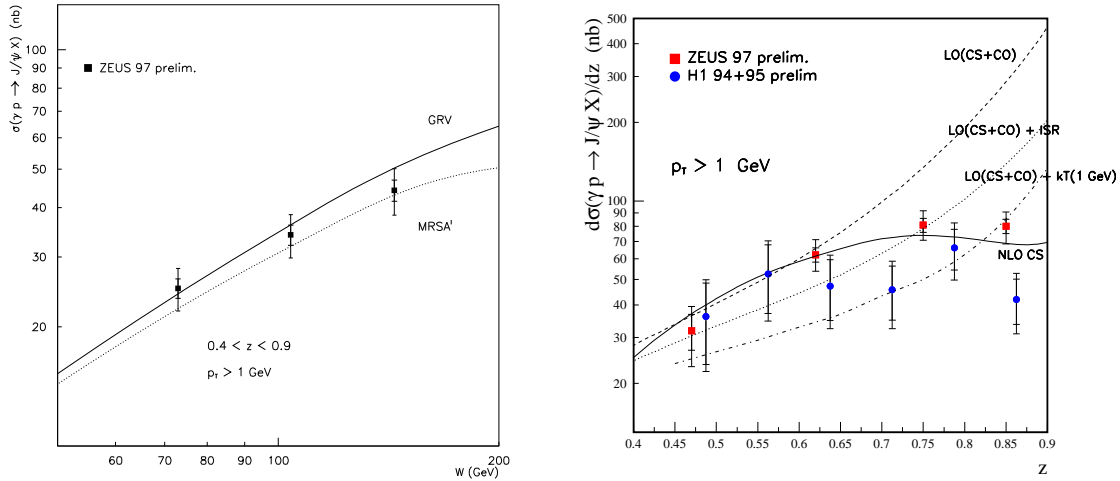


FIGURE 10. Inelastic J/ψ photoproduction: a) cross section as function of $W_{\gamma p}$ for $0.4 < z < 0.9$ and $p_T > 1$ GeV. The lines correspond to the NLO predictions from [13] with GRV or MRSA' [20] parton density functions ($m_c = 1.4$ GeV and $\Lambda_{QCD} = 300$ MeV). b) $d\sigma/dz$ for $50 < W_{\gamma p} < 180$ GeV and $p_T > 1$ GeV. The NLO computation is shown as a solid line. The dashed and dotted lines are given by the sum of the colour-singlet and the colour-octet leading order calculations performed in [15] and in [16]. The latter include estimates of higher order QCD corrections due to initial state radiation.

The corresponding direct LO cross section from the AROMA [10] simulation is 0.19 nb, roughly a factor 5 lower. The fraction of c quarks determined from this analysis leads to the same cross section for $ep \rightarrow ec\bar{c}X$ as previously determined from analysis of D^* production [11].

Inelastic J/ψ production

New data on charmonium (J/ψ , ψ') and Υ production have been presented by H1 and ZEUS [1a]. Here we will concentrate on “inelastic” J/ψ production as opposed to the diffractive processes which dominate the cross section at low Q^2 . Inelastic J/ψ production could at lower $W_{\gamma p}$ (fixed target regime) be well described by the Colour Singlet Model (CSM). For HERA the CSM cross section calculations are available in NLO [13].

As is well known the CSM fails to describe charmonium production in $p\bar{p}$ collisions at high p_T [12]. Colour octet contributions have been proposed for an adequate description. The NRQCD factorisation approach (NRQCD = Non Relativistic QCD) describes any process $A + B \rightarrow J/\psi + X$ as a sum over colour singlet and colour octet contributions.

Whereas the transformation of a colour singlet 3S_1 state into a J/ψ can be calculated using the measured semileptonic decay width, the transition of a colour octet

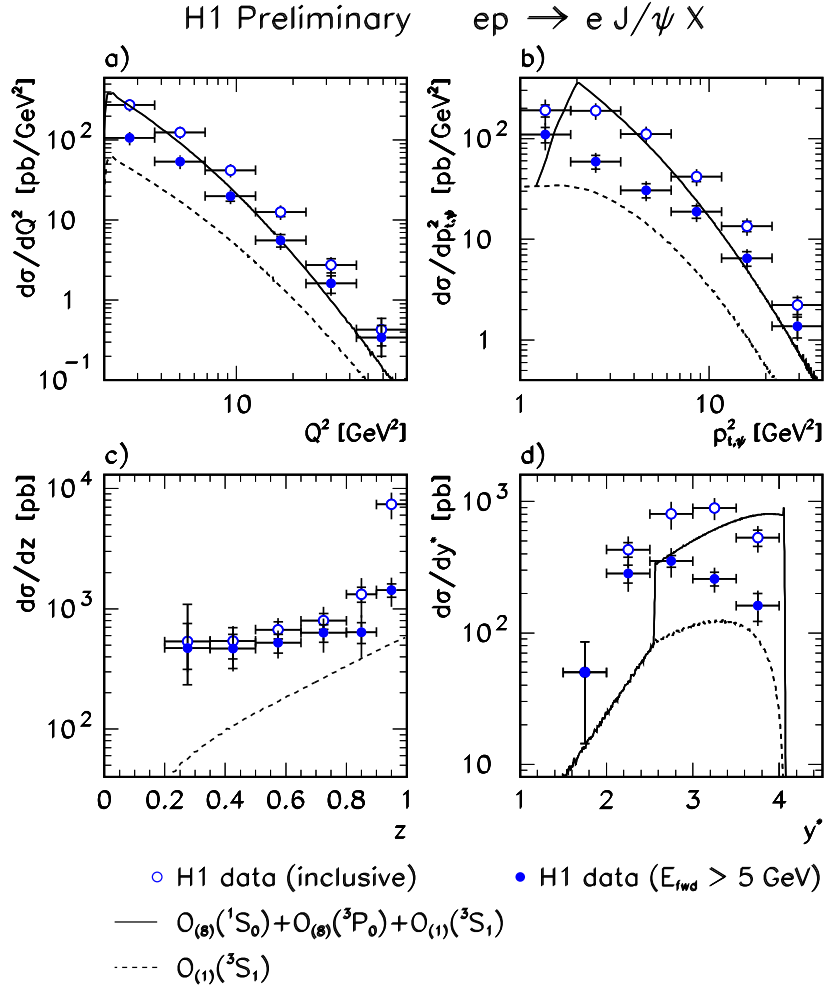


FIGURE 11. Differential cross sections for the inclusive (open points) and inelastic ($E_{fwd} > 5$ GeV, black points) $ep \rightarrow e J/\psi X$ process. a) $d\sigma/dQ^2$, b) $d\sigma/dp_{t,\psi}^2$, c) $d\sigma/dz$ and d) $d\sigma/dy^*$. The curves are predictions [17] within the NRQCD factorization approach for the colour singlet contribution (dashed) and the sum of singlet and octet contributions (full line).

state to J/ψ is non-perturbative and at present not calculable. Therefore predictions for the cross section at HERA use the non perturbative transition matrix elements extracted from the CDF data.

The ZEUS collaboration has updated their photoproduction data [1d]. The results for the γp cross section as function of $W_{\gamma p}$ and of z are shown in fig. 10. The data agree well with the next to leading order pQCD calculation in the color singlet model [13]. The variable z is defined as $z = \frac{P_\psi \cdot P}{P \cdot q} \approx \frac{E_\psi}{E_\gamma}$ where the latter approximation holds in the proton rest frame. In fig. 10 b in addition to the CSM in NLO calculations using the NRQCD/factorisation approach [14–16] are shown. The up-

per curve was calculated in LO using the transition matrix elements extracted from CDF data in LO and shows a strong rise towards high z values. The lower curves also take into account higher orders *approximately* as explained in refs. [14–16]. Doing so leads to modifications in the non perturbative matrix elements and/or in the cross sections themselves. The net effect is a decrease of the predicted rise at high z .

H1 has for the first time determined the cross sections for inelastic J/ψ production at $Q^2 > 2 \text{ GeV}^2$ [1d]. The results are shown in fig. 11. Two data sets are shown, a completely inclusive one (open points) and one where the diffractive contributions have been removed by a cut on the energy in the forward region of the detector as suggested by Fleming and Mehen [17], whose LO calculations are shown for comparison. The data are seen to be far above the CS contributions. The magnitude of the data is reproduced better taking into account colour octet contributions. The shape of the latter leaves, however, much room for improvement, in particular in the rapidity y^* in the $\gamma^* p$ center of mass system. Note that the NRQCD calculations are performed at the parton level, no smearing due to the transition into J/ψ is taken into account.

Summary

Due to increased statistics detailed analyses of heavy flavour production in ep collisions are performed in a variety of channels and kinematic regions. $b\bar{b}$ production was observed for the first time in photoproduction via semi-muonic decay of the b -quark. The cross section was found to be considerably larger than the leading order predictions for the direct process.

In the range $2 \lesssim Q^2 \lesssim 130 \text{ GeV}^2$ cross sections and the charm contribution to F_2^c are determined and found to agree with next to leading order predictions. In photoproduction the validity of different approaches to calculate next to leading order corrections is being studied in various kinematic regions.

Since photon gluon fusion is the dominant process a direct determination of the gluon density in the proton was carried out in DIS and in the photoproduction regime. The result agrees with the indirect determinations from scaling violations.

Inelastic J/ψ production is studied in photoproduction and DIS and is well described in photoproduction by the color singlet model alone in next to leading order. In DIS the data have been compared to LO color singlet and color octet predictions (at parton level). In the latter rough agreement in absolute normalisation is found, while the color singlet model reproduces the shape of the data slightly better.

Acknowledgement I wish to thank the organisers for a very pleasant and fruitful meeting and my colleagues at ZEUS and H1 for supplying their data and for discussions.

REFERENCES

1. Contributed papers to International Conference on High Energy Physics, ICHEP98, Vancouver, July 1998.
<http://www-h1.desy.de/h1/www/publications/conf/list.vancouver98.html>
and <http://www-zeus.desy.de/conferences98/ichep98papers/index.html>
a) ZEUS Coll., contr. paper 791 (Υ), 792 (J/ψ), H1 Coll., contr. paper 572 ($J/\psi, \psi(2s)$), 574 (Υ)
b) H1 Coll., contr. paper 538, 540; ZEUS Coll., contr. papers 768, 772
c) H1 Coll., contr. paper 575
d) ZEUS Coll., contr. paper 814; H1 Coll., contr. paper 573
2. Jung H., *Comp. Phys. Commun.* **86**, 147 (1995)
3. Harris B.W., hep-ph/9608379; DESY 97-111, FSU-HEP-970527, May 1997; *Nucl. Phys.* **B452**, 109 (1995); *Phys. Lett.* **B353**, 535 (1995)
4. Frixione S. et al., *Phys. Lett.* **B348**, 633 (1995); *Nucl. Phys.* **B454**, 3 (1995)
5. Kniehl B.A. et al., *Z. Phys.* **C76**, 689 (1997);
Binnewies J. et al., DESY 97-241, hep-ph/9712482, *Z. Phys.* **C76**, 677 (1997)
6. Cacciari M. et al., *Phys. Rev.* **D55**, 2736 (1997); *ibid.* 7134
7. ZEUS Coll., J. Breitweg et al., DESY 98-085, hep-ex/9807008
8. Chekelian V., DESY 97-248 (1997)
9. Nason P., Dawson S., and Ellis R.K., *Nucl. Phys.* **B303**, 607 (1988);
Ellis R.K. and Nason P., *Nucl. Phys.* **B312**, 551 (1989);
Smith J. and Van Neerven W.L., *Nucl. Phys.* **B374**, 36 (1992)
10. Ingelman G., Rathsman J., Schuler G.A., *Comput. Phys; Commun.* **101**, 135 (1997)
11. H1 Coll., *Nucl. Phys.* **B472**, 32 (1996)
12. CDF Coll., Abe F. et al., *Phys. Rev. Lett.*, **69**, 3704 (1992); *ibid.* **79**, 572 (1997);
DØ Coll., Abachi S. et al., *Phys. Lett.* **B370**, 239 (1996)
13. Krämer M., *Phys. Lett.* **B348**, 657 (1995); *Nucl. Phys.* **B459**, 3 (1996)
14. Beneke M. and Krämer M., *Phys. Rev.* **D55**, 5269 (1997);
Kniehl B.A. and Kramer G., *Phys. Rev.* **D56**, 5820 (1997); **B413**, 416 (1997);
Beneke M., Rothstein I.Z. and Wise M.B., *Phys. Lett.* **B408**, 373 (1997)
15. Cano-Coloma B. and Sanchis-Lozano M.A., *Nucl. Phys.* **B508**, 753 (1997)
16. Sridhar K., Martin A.D., Stirling W.J. DTP-98-30 (1998), hep-ph 9806253
17. Fleming S. and Mehen T., *Phys. Rev.* **D57**, 1846 (1998)